Molecular Ecology (2005) **14**, 1025–1044 doi: 10.1111/j.1365-294X.2005.02472.x

Range expansions in the flightless longhorn cactus beetles, *Moneilema gigas* and *Moneilema armatum*, in response to Pleistocene climate changes

CHRISTOPHER IRWIN SMITH* and BRIAN D. FARRELL
Museum of Comparative Zoology, Harvard University, Cambridge, MA 02138

Abstract

Pollen cores and plant and animal fossils suggest that global climate changes at the end of the last glacial period caused range expansions in organisms indigenous to the North American desert regions, but this suggestion has rarely been investigated from a population genetic perspective. In order to investigate the impact of Pleistocene climate changes and glacial/interglacial cycling on the distribution and population structure of animals in North American desert communities, biogeographical patterns in the flightless, warm-desert cactus beetles, *Moneilema gigas* and *Moneilema armatum*, were examined using mitochondrial DNA (mtDNA) sequence data from the cytochrome oxidase I (COI) gene. Gene tree relationships between haplotypes were inferred using parsimony, maximum-likelihood, and Bayesian analysis. Nested clade analysis and coalescent modelling using the programs MDIV and FLUCTUATE were used to identify demographically independent populations, and to test the hypothesis that Pleistocene climate changes caused recent range expansions in these species. A sign test was used to evaluate the probability of observing concerted population growth across multiple, independent populations. The phylogeographical and nested clade analyses reveal a history of northward expansion in both of these species, as well as a history of past range fragmentation, followed by expansion from refugia. The coalescent analyses provide highly significant evidence for independent range expansions from multiple refugia, but also identify biogeographical patterns that predate the most recent glacial period. The results indicate that widespread desert environments are more ancient than has been suggested in the past.

Keywords: Cerambycidae, Chihuahuan Desert, coalescent analysis, FLUCTUATE, MDIV, nested clade analysis, phylogeography, Sonoran Desert

Received 12 August 2004; revision received 29 October 2004; accepted 10 December 2004

Introduction

The question of whether the Pleistocene ice ages played a significant role in shaping diversity within and between species has been debated for more than a century (Darwin 1859; Wallace 1862; Mayr 1942). Whereas glacial refugia and recent recolonization have often been proposed, conclusive evidence has frequently been lacking, and the extent to which Pleistocene range shifts have been of evolutionary significance remains uncertain (Klicka 1999; Knapp & Mallett 2003; Lessa *et al*. 2003; Wilf *et al*. 2003). The controversy persists in part because of the tremendous difficulty of proving causation in an evolutionary context. To make a truly compelling case for Pleistocene refugia and postglacial range changes, it is necessary to demonstrate not only that range changes have occurred, and that they were contemporaneous with climate changes and glaciation, but also that the demographic events in question were actually driven by climate change.

Although recent advances in molecular systematics, coalescent theory, and molecular clocks have made it easier to infer biogeographical histories within species, demonstrating a causal link between global climate changes and demographic changes in a particular taxon remains quite difficult. Some authors have used multiple independent comparisons between sister groups to test hypotheses

Correspondence: Christopher Irwin Smith, *Present address: Department of Biological Sciences, University of Idaho, Moscow, Idaho 83844. Fax: 208-885-7905; E-mail: csmith@uidaho.edu

about the evolutionary process, such as whether the origin of a particular feature may promote diversification (Mitter *et al*. 1988; Farrell *et al*. 1991; Farrell 1998; Issac *et al*. 2003), but when examining the demographic history of a single taxon, independent iterations of that history are rarely available.

The arid regions of western North America, however, present an unusually promising context in which to explore the consequences of Pleistocene climate changes and glacial/interglacial cycling on terrestrial organisms. The region's complex topography has created many isolated populations and potential refugia (Riddle *et al*. 2000a, b) that may provide multiple independent observations of the effect of climate change on distribution. Additionally, hot, dry climates have allowed the preservation of ancient plant and animal matter in packrat middens, providing a rich source of palaeoenvironmental data (Van Devender 1990a, b; Thompson & Anderson 2000). These data suggest that many of the plants and animals characteristic of modern desert ecosystems survived ice age temperature and rainfall regimes in refugia on the edge of the Sea of Cortez in Sonora, Mexico and in continental depressions near the continental divide in Chihuahua, Mexico (Van Devender & Burgess 1985; Wells 1977). There is further evidence that many of these groups have undergone recent (i.e. Holocene-aged) range expansions and reached their current distributions only during the last 10 000 years (Van Devender 1990a, b; Elias & Van Devender 1992; MacKay & Elias 1992; Morafka *et al*. 1992; Van Devender & Bradley 1994; Elias *et al*. 1995; Thompson & Anderson 2000).

Terrestrial arthropods from these regions offer particular promise for population genetic studies of range expansion. Analyses of insects and other arthropods preserved in packrat middens from the Bolson de Mapimi in the Chihuahuan Desert indicate that this region may have served as a refugium for many desert taxa (Elias *et al*. 1995), and the remains of ants similarly preserved suggest that desert-dwelling species did not achieve their current distributions until 2500 yr BP (MacKay & Elias 1992). Additionally, because of the poor dispersal ability of many of these organisms, it is likely that they may retain a signature of past distribution changes in their population genetic and phylogeographical relationships. Indeed, recent work has identified population genetic evidence of range expansions in desert arthropods (Ayoub & Riechert 2004), and other recent studies suggest that populations of montane, cool-climate insects experienced range fragmentation and isolation during the Pleistocene interglacials (Smith & Farrell in review).

Here, we examine mitochondrial DNA (mtDNA) sequence data and phylogeographical patterns from two species of flightless cactus beetles endemic to desert scrublands occurring in the U.S./Mexico border regions. *Moneilema gigas* LeConte occurs in Sonoran Desert scrub and tropical deciduous forest, ranging from central Arizona, southwards to the southern edge of Sonora, Mexico. *Moneilema armatum* LeConte occurs in the Chihuahuan Desert, from north-central New Mexico, eastwards to the Gulf Coast, and southwards to Zacatecas and Veracruz, Mexico. Based on their distribution and the packrat-midden evidence for range expansions in desert organisms since the end of the last glacial, it seems reasonable to suppose that these insects may show population genetic evidence of recent expansions from refugia.

To test the hypothesis that these animals have undergone range expansions, we examined phylogeographical patterns in these species using phylogenetic and nested clade analyses (NCAs). We then used coalescent analyses to identify demographically independent, genetically isolated groups, infer divergence times between these groups, and test whether each of these groups have undergone population growth. Finally, treating each of these groups as independent observations, we used simple statistical methods to test the hypothesis that common demographic changes across populations were driven by postglacial climate changes.

Materials and methods

Selection of study sites and specimen collections

Collection sites were identified by consulting previous collections data in published accounts (Raske 1966; Linsley & Chemsak 1984) and by examining museum specimens at the Museum of Comparative Zoology at Harvard, the University of Arizona insect collection, the Essig Museum at UC Berkeley, the California Academy of Sciences, and the Instituto de Biología at the Universidad Nacional Autónoma de México (UNAM). Additionally, biotic community maps (Brown 1994) and published accounts of palaeovegetation in the region (Van Devender 1990a, b; Elias & Van Devender 1992; Van Devender & Bradley 1994) were consulted to identify potential new populations and determine which would be most informative in reconstructing Pleistocene climate changes.

Ninety-eight specimens of *Moneilema gigas* were collected from 26 locations across the species' range (See Table 1a). Collection localities in the United States included the Santa Cruz, San Pedro, and Altar river valleys in southeastern Arizona, the Maricopa Mountains and the upper Gila River valley in central Arizona, and the Ajo Mountains in southwestern Arizona. Mexican collection localities included several locations from along the coast of the Sea of Cortez, as well as populations from the Rio Sonora, Rio Yaqui, and Rio Mayo river basins. These locations included populations from both the current northern edge of the Sonoran Desert, and a number of populations from within putative desert refugia on the coast and at low-elevation sites in southwestern Arizona.

Fifty-four individuals of *Moneilema armatum* were collected from 16 locations across New Mexico, west Texas, and northeastern Mexico (See Table 1b). Collection localities in

Table 1a Collection localities for *Moeilema gigas*

Population no.	Name	Location	Coordinates	Haplotypes sequenced	GenBank Accession nos
1	Alamos Monte	Southeast of Alamos, Sonora, on the road towards the Rio Cuchijaqui	26°59′00″N 108°54′12″W	*M. gigas 238.1, 238.2, 238.3*	AY708330–AY708332
2	San Carlos, Sonora	In the town of San Carlos, Sonora	27°50′00″N 110°54′00″W	*M. gigas 234.1, 234.2, 234.3, 240.1, 240.3, 240.4*	AY708326–AY708328; AY708333–AY708335
3	Las Guásimas	Mexico Hwy 15 east of Guaymas, Sonora, Mexico	27°54′24″N 110°34′24″W	*M. gigas 229.1, 229.2*	AY708324, AY708325
4	Playa Del Sol	Mexico Hwy 15, 20 km east of Guaymas, Sonora, Mexico	27°54′24″N 110°45′00″W	*M. gigas 513.1*	AY708366
5	San Nicolas, Sonora	260 km southeast of Hermosillo, Sonora, Near intersection with road to Ciudad Obregón	28°25′00″N 109°15′00″W	*M. gigas 516.1, 516.3, 519*	AY708367–AY708368
6	Moctezuma, Sonora	160 km northeast of Hermosillo, near Moctezuma River	29°30′00″N 109°30′00″W	*M. gigas 496.1, 496.2, 525.1, 525.2*	AY708364, AY708365, AY708370, AY708371
7	Ures, Sonora	60 km northeast of Hermosillo	29°30′00″N 110°30′00″W	*M. gigas 489.1, 489.2, 489.3, 491.1, 491.2, 492.1*	AY708358–AY708363
8	Mazocahui, Sonora	104 km northeast of Hermosillo, near road to Cananéa	29°31′43″N 110°09′15″W	*M. gigas 487.1*	AY708353
9	Husabas, Sonora	200 Km northeast of Hermosillo, Sonora near Rio Bavispe	29°50′00″N 109°25′00″W	*M. gigas 488.1, 488.2, 488.4, 488.5*	AY708354–AY708357
10	Km 100	Mexico Hwy 15, 100 km north of Hermosillo, Sonora, Mexico	30°00′00″N 111°08′00″W	*M. gigas 221.2, 224, 228.1, 228.2, 228.3*	AY708319–AY708323
11	Cholla Bay, Sonora	Cholla Bay, west of Puerto Peñasco, Sonora, Mexico	31°15′00″N 114°40′00″W	*M. gigas 218.1, 218.2, 218.3, 218.4, 219.1, 219.2, 219.3*	AY708310–AY708316
12	Sonoita, Sonora	Off Mexico Hwy 2, just east of Sonoita, Sonora, Mexico	31°41′18″N 112°50′48″W	*M. gigas 203.1, 203.2, 203.3, 220.1, 220.2*	AY708305–AY708307; AY708317, AY708318
13	Sheriff's Mesa, Arizona	Between Amado and Arivaca on Batamote Road., Santa Cruz County, Arizona	31°45′00″N 111°11′00″W	*M. gigas 146.1, 146.2*	AY708294, AY708295
14	Baboquivari, Arizona	Brown Canyon, east of Baboquivari Mountain, Pima County, AZ	31°45′00″N 111°30′00″E	*M. gigas WM01, WM02*	AY708373, AY708374
15	Florida Canyon, Arizona	Santa Rita Mountains, above Santa Rita Experimental Range Station, Santa Cruz County, Arizona	31°46′00″N 110°51′00″W	*M. gigas 012, 014, 016, 019, 024, 039, 050*	AY708279–AY708285
16	Box Canyon, Arizona	Box Canyon Road between Greaterville and the Santa Rita Experimental Range Station, Santa Cruz County, Arizona	31°47′00″N 110°50′18″W	*M. gigas 301.1, 301.2, 304, 305.1, 305.2, 308, 310.1, 312.1, 312.2, 317.2*	AY708336, AY708337, AY708342–AY708349

Table 1a *Continued*

Population no.	Name	Location	Coordinates	Haplotypes sequenced	GenBank Accession nos
17	Puerto Blanco Mts, Arizona	Off Organ Pipe Loop Drive, Organ Pipe National Monument, Pima County, Arizona	31°59′06″N 112°50′20″W	*M. gigas 115*	AY651016
18	Bull's Pasture, Arizona	Bull's Pasture in the Ajo Mountains, Organ Pipe National Monument, Pima County, Arizona	32°00′55″N 112°41′36″W	*M. gigas 156.1, 156.2, 158*	AY708297–AY708299
19	Altar Valley, Arizona	Intersection of Arizona Hwy. 86 and 286 Pima County, AZ	32°03′00″N 111°19′00″W	*M. gigas 139, 145*	AY708292, AY708293
20	Tucson, Arizona	Near Intersection of Grant and Country Club, Tucson, Pima County Arizona	32°15′00″N 110°56′00″W	*M. gigas 123*	AY708290
21	Black Mt, Arizona	Black Mountain, South of Ajo, Pima County, Arizona	32°20′32″N 112°44′30″W	*M. gigas 130, 147*	AY708291, AY708296
22	Catalina State Park, Arizona	Catalina State Park Group Use Area, Pima County, Arizona	32°26′00″N 110°55′00″W	*M. gigas 046, 071, 075*	AY651015, AY708286, AY708286
23	Biosphere II, Arizona	Biosphere II Center, Pinal County, Arizona	32°34′20″N 110°51′30″W	*M. gigas 160.1, 169, 170*	AY708300, AY708302, AY708303
24	Oracle, Arizona	Arizona Trail off Mt. Lemon Road, Oracle, Pinal County Arizona	32°36′30″N 110°45′00″W	*M. gigas 207, 211.2*	AY708308, AY708309
25	Tiger Mine, Arizona	Off Az HWY 77, northeast of Oracle, Arizona, Pinal County, Arizona	32°38′18″N 110°44′20″W	*M. gigas 161*	AY708301
26	Table Mts, Arizona	South of Interstate 8, near Table Top Wilderness, Pinal County, Arizona	32°39′54″N 112°12′36″W	*M. gigas 116.1, 116.2, 178*	AY708288, AY708289, AY708304
27	Willow Springs Road, Arizona	Off Az Hwy 77, southwest of Oracle, Arizona	32°44′54″N 110°53′50″W	*M. gigas 303.1, 303.2, 303.3, 319.1, 319.2*	AY708339–AY708341; AY708351, AY708352
28	Dripping Springs, Arizona	Dripping Springs Canyon, Off Hwy 77, Pinal Mountains, Gila County, Arizona	33°12′00″N 110°48′15″W	*M. gigas 318*	AY708350

the United States included several populations from the continental divide region of southwestern New Mexico, the Rio Grande valley in central New Mexico, the Tularosa Valley north of White Sands Missile range, and the Hueco, Franklin, and Davis mountains in extreme western Texas. Collections in Mexico included locations in Durango and Chihuahua in the central plateau region, as well as populations from the plains of Tamaulipas, and the eastern edge of the Bolson de Mapimi. Collection locality coordinates for both species were recorded using a hand-held Garmin GPS 12, or E-map GPS unit (See Table 1a and 1b).

Genetic analysis

Specimens were selected for sequencing to obtain representative samples from across the species' ranges. Several outgroup taxa were also selected for sequencing, including specimens of *Moneilema appressum*, *M. semipunctatum*, *M. michelbachari* and the lamiine cerambycid beetle, *Coenopoeus palmeri*, all of which were collected by the authors.

Whole genomic DNA was isolated from these individuals using a salting-out procedure (Sunnucks & Hales 1996). Genetic material was resuspended in 50 μL of 1× buffer

Table 1b Collection localities for *Moneilema armatum*

Population no.	Name	Location	Coordinates	Haplotypes sequenced	GenBank Accession nos
29	10 de Octubre, Durango	Mexico Highway 45, west of San Juan del Rio, Durango, Mexico	24°43′60″N 104° 39′00″W	*M. armatum 397.1, 408.1*	AY704262, AY704269
30	Monterrey, Nuevo Leon	Mexico Hwy 53, 7 km northwest of Monterrey, Nuevo Leon, Mexico	25°40′00″N 100°19′00″W	*M. armatum 540.2*	AY704227, AY704228
31	China, Nuevo Leon	Mexico Hwy 40, near China Resevoir, Nuevo Leon, Mexico	25°41′00″N 99°13′60″W	*M. armatum 541, 542.2*	AY704265, AY704266
32	Reynosa, Tamaulipas	Mexico Hwy 40, 10 km south of Reynosa, Tamaulipas	26°01′00″N 98°13′00″W	*M. armatum 544.2, 544.4*	AY704267, AY704268
33	Monclova, Coahuila	Northwest of Monclova, Coahuila de Zaragoza, Mexico	26°54′00″N 101°25′00″W	*M. armatum 537.1*	AY704263
34	Medley Draw, Texas	Texas Rt 166 near wind farms east of Fort Davis, Jeff Davis County, Texas	30°31′50″N 104°11′59″W	*M. armatum 135.2*	AY704226
35	Bear Mt, Texas	Davis Mountains, Jeff Davis County, Texas	30°43′27″N 104°13′32″W	*M. armatum 138, 140*	AY704227, AY704228
36	Cox Mts, Texas	Off County Hwy 1111, north of Sierra Blanca, Hudspeth County, Texas	31°16′45″N 105°13′48″W	*M. armatum 143, 144.1, 144.2*	AY704229–AY704231
37	Franklin Mts, Texas	Franklin Mountains in County Road 375 Loop, north of El Paso, El Paso County, Texas	31°52′33″N 106°29′34″W	*M. armatum 359.1, 359.2, 359.3, 359.4, 359.5*	AY704242–AY704246
38	Antelope, New Mexico	New Mexico Hwy 9, east of Animas, New Mexico near Continental Divide, Hidalgo Cty, New Mexico	31°55′30″N 108°43′00″W	*M. armatum 354.1, 354.2, 354.3, 354.5*	AY704238–AY704241
39	Old Hachita, New Mexico	Old Hachita Road and New Mexico Hwy 9, West of Hachita, Grant County, New Mexico	31°55′48″N 108°24′12″W	*M. armatum 128*	AY704220
40	Tres Hermanas, New Mexico	Near Tres Hermanas Mountains off New Mexico Hwy 11, south of Deming, Luna County, New Mexico	31°57′15″N 107°45′40″W	*M. armatum 353.1, 353.2, 353.3, 353.4, 363.1, 363.2, 363.3, 363.6*	AY704234–AY704237; AY704247–AY704250
41	Hueco, Texas	County Road 001 and US 180, near Hueco, Hudspeth County, Texas	31°58′00″N 105°58′00″W	*M. armatum 252.1, 252.2*	AY704232, AY704233
42	Doña Ana Mts, New Mexico	Doña Ana Peak, off County road 64, north of Las Cruces, Doña Ana County, New Mexico	32°28′24″N 106°45′54″W	*M. armatum 111.1, 111.2, 111.3*	AY704217–AY704219
43	Sierra Las Uvas, New Mexio	Off New Mexico Hwy 185, South of Hatch, Doña Ana County, New Mexico	32°32′29″N 107°07′38″W	*M. armatum 131.1, 131.2*	AY704221, AY704222
44	Valley of Fire, New Mexico	Off US 380, northeast of Carrizozo, Lincoln County, New Mexico	33°40′55″N 105°55′05″W	*M. armatum 133, 134.1, 134.2*	AY704223–AY704225
45	Correo, New Mexico	Interstate 40, Exit 126 near Correo, New Mexico, Cibola County, New Mexico	34°59′27″N 107°05′54″W	*M. armatum 373.1, 373.2, 373.3, 373.4, 376.4, 376.6*	AY704251–AY704256
46	Bernalillo, New Mexico	Interstate 25 at exit 242, Bernalillo, Sandoval County, New Mexico	35°18′58″N 106°31′54″W	*M. armatum 378.1, 378.2, 378.3, 378.4, 378.5*	AY704269–AY704261
47	Granite Gap, New Mexico	Arizona/New Mexico State Line at NMHwy 80. Hidalgo Cty, NM	32°05′20″N 108°58′25″W	*M. armatum 109*	AY651009

TE, and stored at –20 °C until polymerase chain reaction (PCR) amplification. Reactions were performed using a modified version of the procedure described in Palumbi (1996), using 2 μL of undiluted whole genomic template and 2 μL of $MgCl_2$ catalyst in a 50 μL reaction. Reactions used a 52 °C annealing temperature, held for 90 s, and a 60 °C extension temperature, held for 2 min. This procedure was used to amplify a 780-bp sequence of the cytochrome oxidase I (COI) gene between positions 2183 and 2963 of the *Drosophila yakuba* mitochondrial genome. Additionally, for some individuals the first half of the COI gene, between positions 1541 and 2590, was also amplified, giving a combined total of 1422 bases. Primer sequences were obtained from previously published studies (Farrell 2001).

PCR products were visualized using gel electrophoresis, in 1.5 × agarose gels stained with ethidium bromide (EtBr). Successful PCRs were compared with negative controls and with a standard low DNA mass ladder to ensure that only target sequences were amplified and to quantify PCR product concentrations.

PCRs were purified using QIAGEN PCR purification kits (QIAGEN), and purified DNA product was eluted in 50 μL of the QIAGEN elution buffer EB. DNA sequence data were obtained from these amplified sequences using thermal cycle sequencing. Sequencing reactions used ABI Corporation Dye Terminator or Bigdye version 2 reaction mixtures and the same primers that had been used to amplify the target gene region. Amplified DNA was sequenced using both forward and reverse primers, and was analysed by electrophoresis in 1% acrylamide sequencing gels run on an ABI 370 or 377 automated DNA sequencer, or in polymer-filled capillaries in an ABI 3100 capillary sequencer.

Sequence data were analysed using the ABI SEQUENCING ANALYSIS software version 3.4.1 (Applied Biosystems Inc) and visualized using the SEQUENCHER software package versions 3.0 and 4.1 (Gene Codes). Sequences were easily aligned by eye using MACCLADE version 4.03 (Maddison & Maddison 2001), and translated amino acid sequences were compared with known COI sequences from across the class Insecta to ensure sequence homology.

Phylogenetic analysis

Phylogenetic analyses were performed on the University of Idaho's Beowulf cluster which has 44 2.8 GHz dual Intel Corporation processor nodes, and 1.0 GB RAM. All data were analysed using PAUP version 4.0b10 (Swofford 2002), under parsimony and maximum-likelihood optimality criteria. Most parsimonious trees were found by heuristic searches starting with 100 random addition sequences starting from random trees and using tree-bisection–reconnection (TBR) branch swapping; all characters were equally weighted. Support for the relationships found in these searches was evaluated with 100 replicate bootstrap analyses using heuristic searches with 10 addition sequences each, starting from random trees.

Likelihood models that best fit the data set were selected by MODELTEST version 3.06 (Posada & Crandall 1998). Maximum-likelihood-based searches were executed in PAUP using a heuristic search strategy with a single random addition sequence starting from a random tree.

Bayesian analysis

Bayesian analyses of molecular evolution were executed in MRBAYES version 3.0 (Huelsenbeck & Ronquist 2001). Each data set was initially analysed using three independent runs of 5 000 000 generations each, sampling every 100 generations, and employing a general time reversible model with flat priors set for all parameters. Each MRBAYES run used four separate chains; the default settings were used for chain heating. Results of each MRBAYES run were graphed using MS Excel to identify the point at which all estimated parameters reached stationarity. To ascertain whether solution space was adequately sampled, the clade posterior probabilities from a subset of the postburn-in trees in each run were contrasted against one another using the 'compare' feature in MRBAYES. If the correlation between posterior probabilities was less than 0.99, or if the topologies observed in the Bayes consensus trees from different replicates were not identical, then data were reanalysed with progressively longer Markov chains, increasing in 5 000 000 generation increments, until posterior probabilities between runs were at least 99% correlated.

Nested clade analysis

A gene network analysis was computed using the TCS program version 1.13 (Clement *et al*. 2000). The program was set to estimate the upper limit of the number of mutational steps between haplotypes. The resulting gene network was then grouped into one, two, three, four, five and six-step clades by hand, according to the methods described by Templeton *et al*. (1987) and employing special modifications of these rules described in Templeton & Sing (1993) to handle equivocal groupings of haplotypes. To measure the association of geography with the hierarchical structure in the gene network, data were analysed using the GEODIS software package version 2.0 (Posada *et al*. 2000). The input file for GEODIS was created by hand from the nested cladogram following the procedure described in the documentation file for GEODIS; within-clade and nested-clade geographical distances were calculated by GEODIS from the latitude and longitude coordinates for each collection locality (Posada *et al*. 2000). Output from the GEODIS program was interpreted using the inference keys in Templeton (1998, 2004).

Coalescent modelling

Coalescent theory has enabled powerful methods for inferring population genetic parameters, such as effective population size and migration rates, as well as testing hypotheses about demographic histories, such as the recent population expansions that are hypothesized here. In order to evaluate whether the observed biogeographical patterns in these two species are consistent with Pleistocene climate changes, divergence times, migration rates between populations, and rates of population growth within groups of populations were calculated using coalescent modelling.

Because we wished to evaluate the statistical support for population expansion in multiple, demographically independent groups, we sought to identify populations, or groups of populations, that could be treated as distinct entities in coalescent analyses. Conversely, we wished to avoid separate analyses of populations that were not truly independent, as this would overestimate the number of independent data points and erroneously inflate statistical significance. For purposes of this study there are two ways that groups of populations might not be demographically independent with respect to responses to Pleistocene climate shifts: first, if two populations diverged more recently than the Last Glacial Maximum (LGM), then they might both reflect evidence of population growth that occurred prior to their divergence; second, if two populations were exchanging a large number of migrants, then growth in one of these populations might produce the genetic signature of recent population expansion in the other. To deal with these possibilities, we used the MDIV software package developed by Rasmus Nielsen that implements the coalescent model described in Nielsen & Wakeley (2001). Although it was not designed to distinguish discrete populations per se, because this program jointly estimates migration rates and divergence times, with an eye to distinguishing the retention of ancestral polymorphisms from ongoing gene flow, it was ideal for our purposes. Aligned sequence data from pairs of collection localities were used to estimate the parameters 'Θ' (= $2N_e\mu$), M (= $N_e m$ = number of migrants between populations per generation), and T (the divergence time between populations where 1 time unit = N_e generations). These analyses each used a finite sites model, and a 3 000 000 generation Markov chain Monte Carlo (MCMC) with a 500 000 generation burn-in time was used to explore the solution space. M_{max} was set to 3, and T_{max} to 10. The coalescent-scaled parameter T was converted to T_{div} (time in years since two populations diverged) by assuming one generation per year (Raske 1966) and a neutral mutation rate of 1.5% per million years (Myr) (Farrell 2001) according to the formula:

$$T_{div} = T\Theta/(2\mu)$$

Based on the results of all pairwise comparisons in MDIV, sequence data from distinct localities were pooled if estimates of M were significantly greater than 0.1, or if estimates of T_{div} were not significantly greater than 100 000 years ($P = 0.01$; P values for these estimates were calculated by integrating under the posterior distributions output by MDIV.) Although most researchers mark 18 000 BP as the end of the last glacial period, we chose 100 000 BP (the end of the previous interglacial) as a cutoff in order to be conservative in identifying independent groups, and to account for potential errors in estimating divergence times as a result of reliance on a single, non-recombining locus. Populations that diverged more than 100 000 BP and did not show evidence that they were exchanging migrants were considered to be demographically independent with respect to climate change since the LGM, and were analysed separately to test for evidence of population expansion.

The parameter estimates from MDIV were not used for subsequent statistical analysis of population structure because the multiple pairwise contrasts do not represent independent observations. Instead, data from each of the pooled populations for which there was sequence data from at least three individuals were analysed using the program FLUCTUATE (Kuhner *et al*. 1998). The program was used to estimate the parameters Θ (defined above) and 'g' (the exponential rate of population growth or decline relative to the neutral mutation rate). We set the program to compute the Watterson estimate of Θ, and allowed the population to change in size, with an initial value for 'g' set to 0.1. We used 10 short MCMC simulations of 200 generations each, and two long MCMC simulations of 20 000 generations each to explore the solution space. The probability that 'g' ≥ 0 was determined by referring to plots of the likelihood surface output using FLUCTUATE. Following the procedure described in Wares & Cunningham (2001), the FLUCTUATE analyses were repeated five times for each group of pooled populations, and the mean and standard deviation of Θ and 'g' were calculated from the results of these separate runs.

Additionally, because it has been suggested that FLUCTUATE may have an upward bias in measuring population growth rates, we also calculated the more conservative statistic Fu's F_S. Although the F_S was designed as a test of neutrality, it also has utility as a test of population growth, as population expansion produces strongly negative values of F_S (Fu 1997). F_S was calculated using ARLEQUIN version 2.000 (Schneider *et al*. 2000); significance of F_S values were calculated using 1000 simulated samples to produce an expected distribution under constant population size.

The significance of common population genetic patterns across groups of populations was evaluated. The sign of the parameters 'g' and Fu's F_S from each of the groups analysed was recorded, and the probabilities of finding as

many or more groups of populations for which 'g' was positive, or for which F_S was negative, were measured using sign tests (Daniel 1991).

Results

Genetic data

An average of 802 base pairs of mtDNA sequence data was obtained from 98 individuals of *Moneilema gigas* (GenBank Accession nos AY651015, AY651016 and AY708279–AY708372). Fifty-two individuals of *Moneilema armatum* were sequenced, with an average of 712 bp each (GenBank Accession nos AY651009 and AY704217–AY704269). The data from *M. gigas* suggest an empirical transition/transversion ratio of 1.48 and an A-T bias with empirical base frequencies of A: 0.29793 C: 0.13495 G: 0.15214 T: 0.41498. Of the 506 variable sites, 231 were parsimony-informative. Sequence data obtained from *M. armatum* suggest an empirical transition/transversion ratio of 1.66, and an A-T bias similar to that found in *M. gigas*, with empirical base frequencies of A: 0.29851 C: 0.15124 G: 0.15939 T: 0.39086. There were 286 variable sites, of which 150 were parsimony-informative.

Phylogenetic analysis

Parsimony analysis of sequence data from *M. gigas* found 2 000 000 equally parsimonious trees 1612 steps long, which had a consistency index of 0.5676 and a retention index of 0.7474. MODELTEST selected a GTR + I + G model of sequence of evolution for the *M. gigas* data set, and the heuristic search using this model found a single maximum-likelihood tree with a log likelihood score of –10333.45469. In the Bayesian analysis clade, posterior probabilities were 99% correlated between runs after 20 000 000 generations. A 1 000 000 generation burn-in time was selected by examining the point where parameter estimates reached stationarity within each run, and the 190 000 postburn-in trees from each of three runs were combined to compute the Bayes consensus. These trees had an average log likelihood score of –10471. ± 16.

All three optimality criteria selected very similar topologies; the Adams' consensus of the parsimony, Bayes consensus, and maximum-likelihood trees (See Fig. 1 and

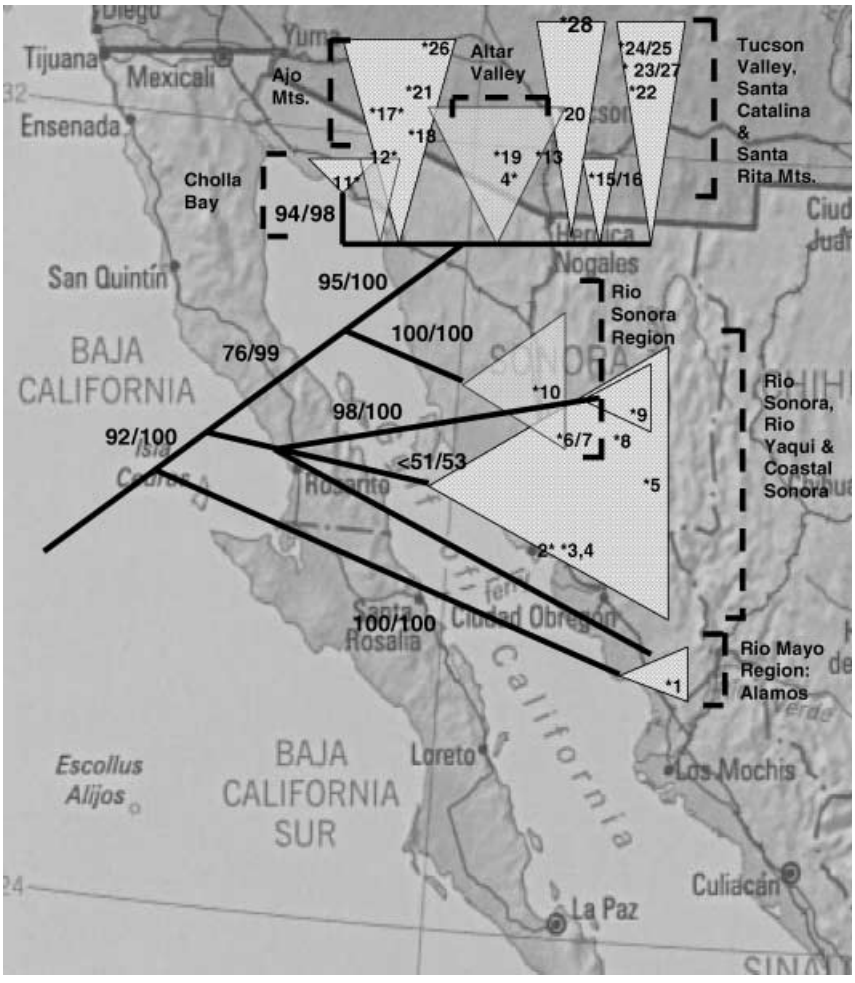

Fig. 1 Phylogeographical patterns in *Moneilema gigas*. The topology is a simplified version of the Adams' consensus tree. Nodal indices are bootstrap supports/Bayes posterior probabilities. Numbers indicate collection localities (Table 1a); boldface labels indicate the regional distribution of each clade. The base map is copyright to the General Libraries of the University of Texas at Austin, and is used with permission.

Supplementary material) finds that sequences sampled from populations in Arizona and the U.S./Mexico border region form a large clade that is derived with respect to populations from southern and central Sonora. This clade had high bootstrap support (95%) and high Bayes posterior probabilities (100%). Within this clade there is evidence for some geographical structuring; the consensus tree identified several clades corresponding to populations from the Santa Catalina Mountains, the Santa Rita Mountains, the Altar Valley, and Cholla Bay on the Sea of Cortez but these were only weakly supported (< 50% bootstrap support). Sequences from the southernmost locality of Alamos, form a basal grade. Sequences drawn from populations in central and coastal Sonora also form a large clade, which is derived with respect to most of the sequences from Alamos, although one sequence from Alamos is ambiguously placed within this group. Finally, sequences from the Hermosillo region near the upper Rio Sonora are strongly supported as the sister group to sequences from Arizona and Cholla Bay in northern Sonora (76% bootstrap support, 99% Bayesian posterior probability).

Parsimony analysis of the sequence data for *M. armatum* found 2 000 000 equally parsimonious trees, 1307 steps long. These trees had a consistency index of 0.5570 and a retention index of 0.8145. MODELTEST selected a GTR + I + G model of sequence evolution, and the heuristic search using this model selected six equally likely trees with a log-likelihood score of −8281.72558. In the Bayesian analysis, clade posterior probabilities were 99% correlated between runs after 10 000 000 generations. 90 000 postburn-in trees from each of three separate runs were combined to compute the Bayes consensus tree. These trees had an average log likelihood score of −8385 ± 12.

The Adams' consensus of the parsimony, Bayes consensus, and maximum likelihood trees (See Fig. 2 and supplemental material) finds support for five major monophyletic lineages within the ingroup. There is a basal split between populations on the east and west sides of the Rio Grande valley, and the monophyly of these two groups was supported by high bootstrap supports (96% and 86%) and high posterior probabilities (100% and 99%). Within the clade containing populations from west of the Rio Grande, there is evidence for three major clades that are strongly supported as monophyletic in both the bootstrap (94–100%) and Bayesian analyses (100% posterior probabilities). The basal-most of these clades includes populations from

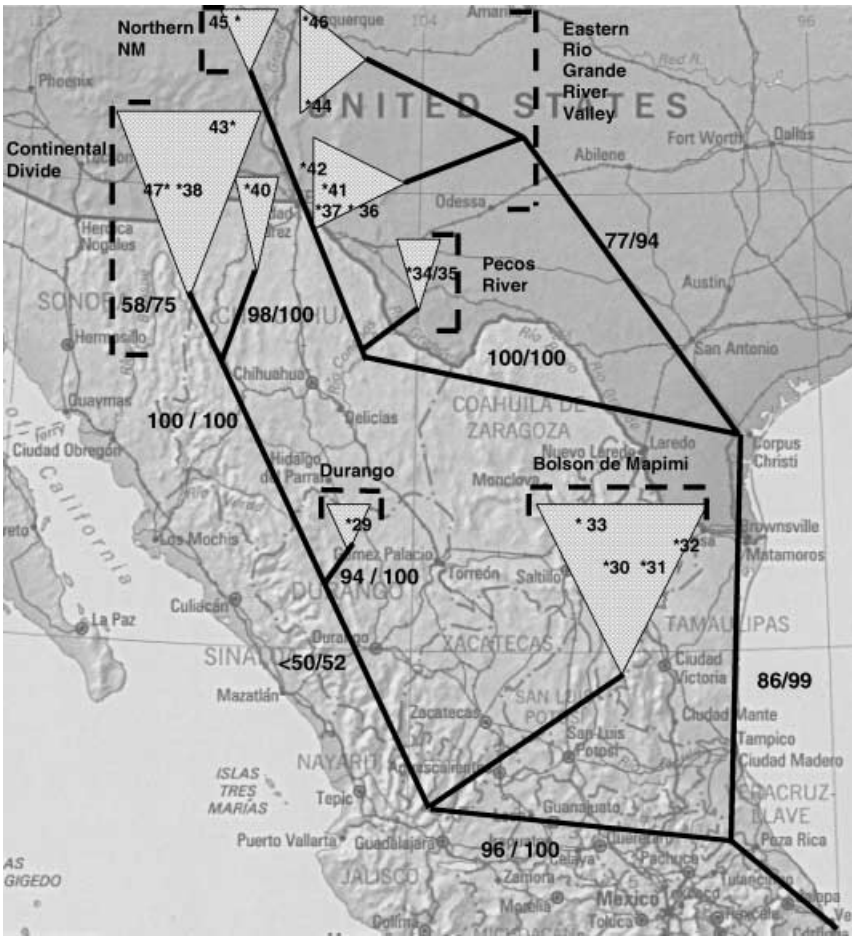

Fig. 2 Phylogeographical patterns in *Moneilema armatum*. The topology is a simplified version of the Adams' consensus tree. Nodal indices are bootstrap supports/Bayes posterior probabilities. Numbers indicate collection localities (Table 1b); boldface labels indicate the regional distribution of each clade. The base map is copyright to the General Libraries of the University of Texas at Austin, and is used with permission.

Table 2 Nested clade analysis (significant clades only)

Species	Clade	Distribution	Chi-squared statistic	*P*	Biogeographical interpretation
M. gigas	3–18	Arizona/northern Sonora	49.11	0.05	Past fragmentation
	5–1	Rio Sonora, Rio Yaqui, Rio Mayo, coastal Sonora	33.86	< 0.0001	Past fragmentation
	5–3	Arizona/northern Sonora	63.47	< 0.0001	Inconclusive
	Total cladogram	*c*	147.03	< 0.0001	Past fragmentation
M. armatum	6–1	Pecos River and eastern Rio Grande valleys, northern New Mexico	44.46	< 0.0001	Contiguous range expansion
	6–2	Bolson de Mapimi, Continental Divide region	16.00	0.001	Insufficient geographic sampling
	Total cladogram	*c*	43.00	< 0.0001	Past fragmentation

central Mexico, including the Bolson de Mapimi and the Mexican Gulf coast. The remaining two groups include populations from Durango, Mexico, and populations from the Continental Divide region of southwestern New Mexico, west of the Rio Grande. These clades are each other's sister groups in the consensus tree, but this relationship is only weakly supported in the Bayesian analysis (52% posterior probability). Among populations from east of the Rio Grande valley there is strong support for a clade containing populations from the Davis Mountains in the trans-Pecos region of west Texas and, oddly, the population from Correo, in northwestern New Mexico. The remaining sequences in this group represent populations from the eastern side of the Rio Grande valley.

Nested clade analysis

The gene network analysis identified 79 haplotypes from *M. gigas*, which were grouped into a single network (Fig. 3a–3h), although two haplotypes from Alamos, Sonora were too divergent to be placed unambiguously within the gene network, and were excluded from subsequent analyses. Grouping the haplotypes into nested clades using the method described in Templeton (1998) found eight four-step clades, three five-step clades and one six-step clade (the total cladogram). Analysis of the spatial distribution of the nested clades using the GEODIS program found significant geographical structure in clades 3–18, 5–1, 5–3, and in the total cladogram (see Table 2). Interpretation of these results using the inference keys in Templeton (1998) and Templeton (2004), found that the structure in these clades is consistent with a past history of fragmentation.

Forty-four haplotypes of *M. armatum* were grouped into four five-step clades, and two six-step clades (Fig. 4). Analysis of the spatial distribution of these nested clades using the GEODIS program found significant geographical structure in clades 6–1, 6–2, and in the total cladogram (see Table 2). Interpretation of these results using the inference key in Templeton (1998) and Templeton (2004) suggests a past history of fragmentation overall, and contiguous range expansion within clade 6–1, which corresponds to populations from east of the Rio Grande. However, inadequate sampling from some areas, particularly the southern

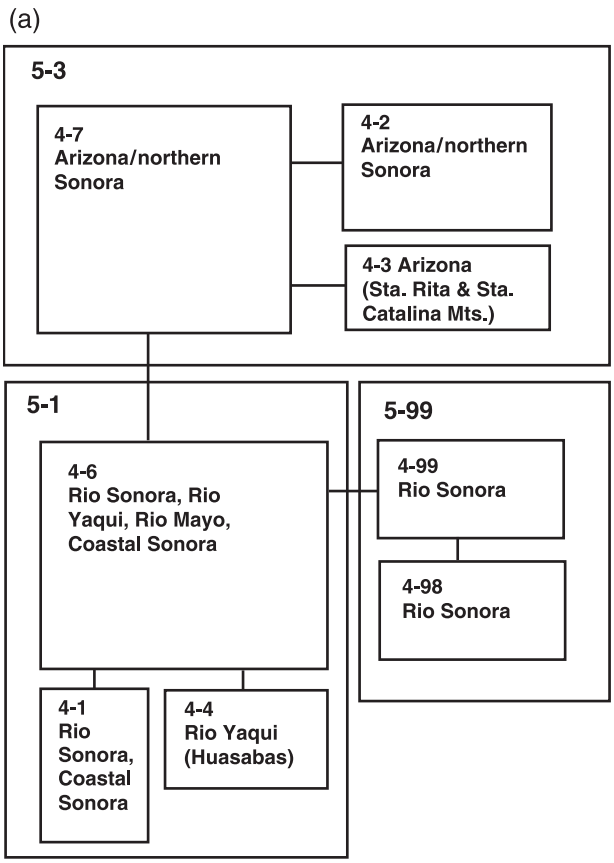

Fig. 3 Nested clades in *Moneilema gigas*. (a) Five-step clades showing distribution of each clade. (b) 2-, 3-, and 4-step clades that contain both genetic and geographical variation. The number of mutational steps between major groups are shown as branch indices. (c) Clade 2–31, detail. (d) Clade 1–30, detail. (e) Clade 2–44, detail. (f) Clade 1–96, detail. (g) Clade 2–18, detail. (h) Clades 2–45 and 2–47, detail.

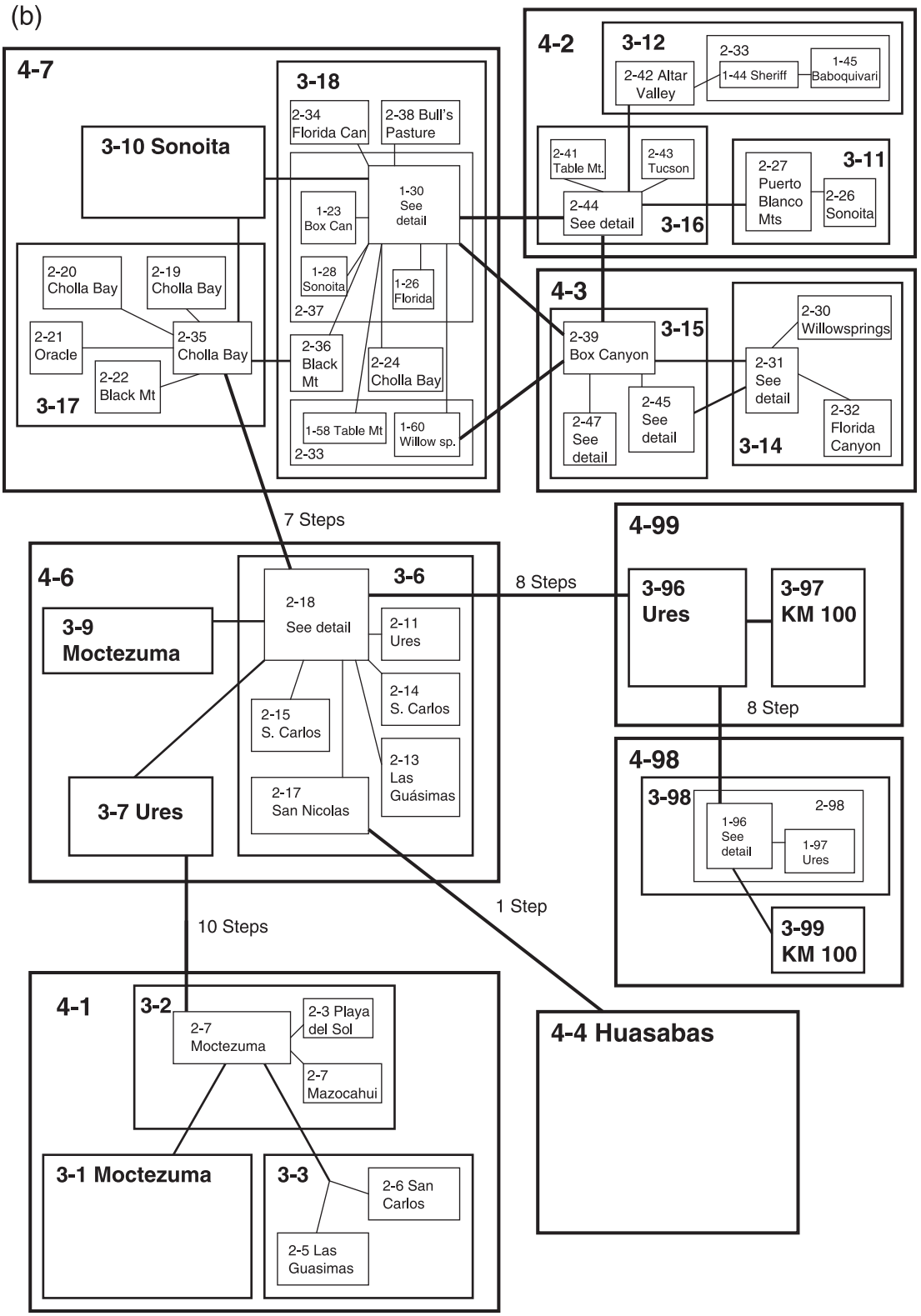

Fig. 3 *Continued*

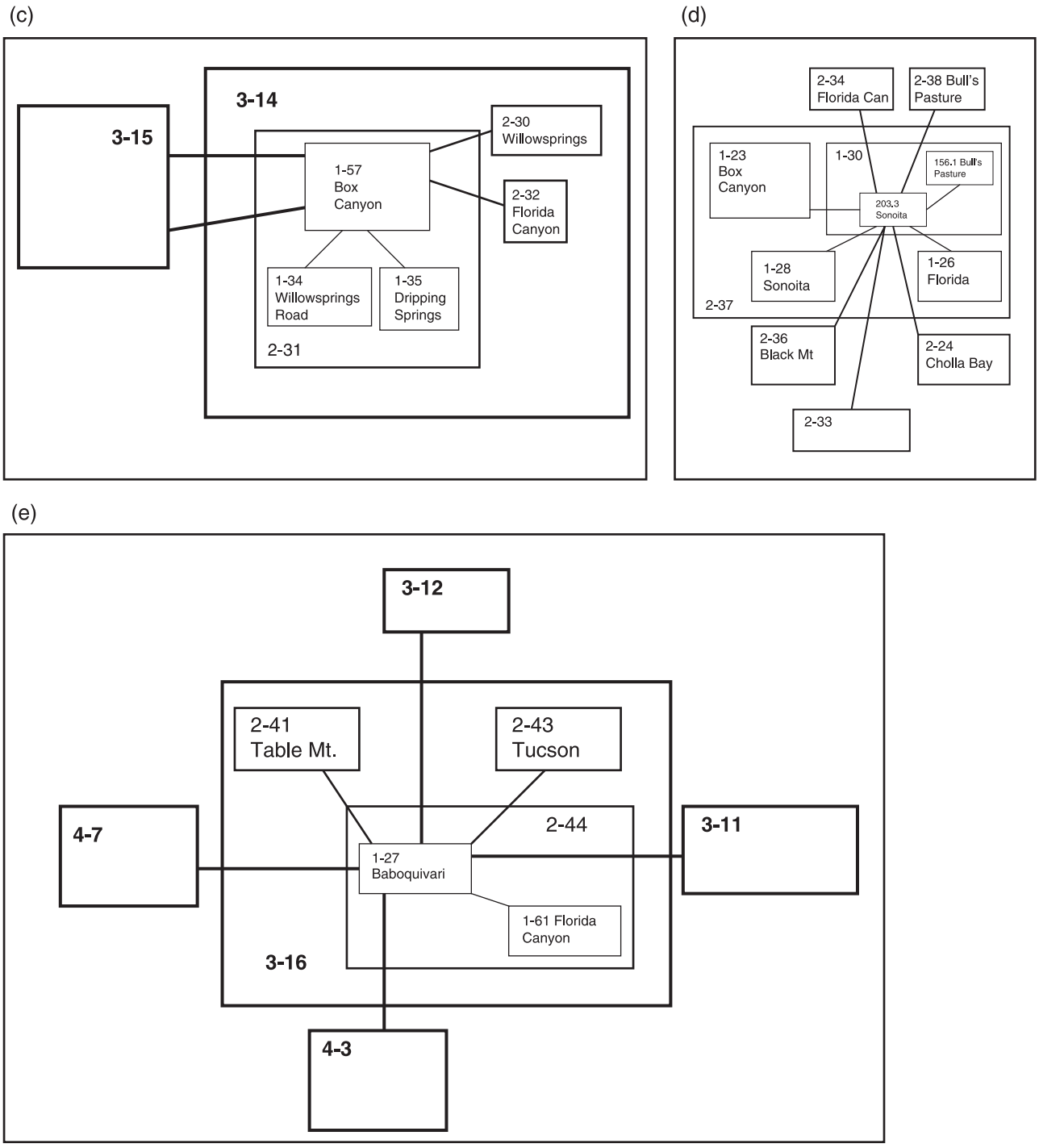

Fig. 3 *Continued*

half of the range valley makes it difficult to distinguish these patterns from isolation by distance (Templeton 1998). Additionally, as with the basal haplotypes in *M. gigas*, two haplotypes from Durango could not be unambiguously connected to the other haplotypes and were excluded from the subsequent analysis.

Coalescent analyses

Estimation of migration rates and divergence times using MDIV identified eight distinct groups of populations within *M. gigas* (See Table 3) and six groups within *M. armatum* (Table 4); these were the same regions

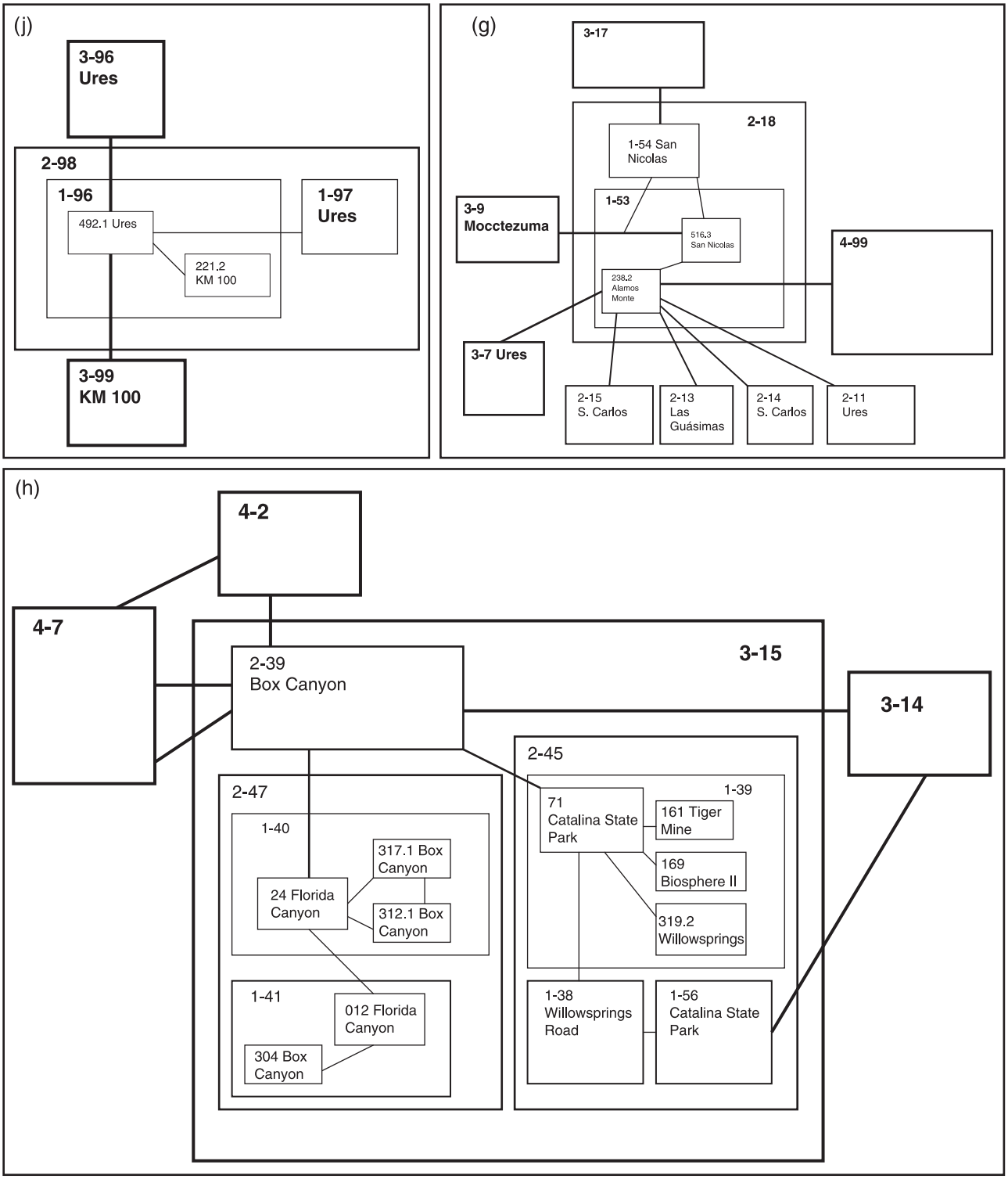

Fig. 3 *Continued*

identified in phylogenetic and nested clade analyses (cf. Figs 1–4). Divergence times between regions varied between 0.15 and 2.0 Myr in *M. gigas*, and between 0.9 and 5.0 Myr in *M. armatum*.

The estimates of migration rates and divergence times were generally concordant, that is, the highest migration rates between collection localities tended to be between populations that had also diverged quite recently. However,

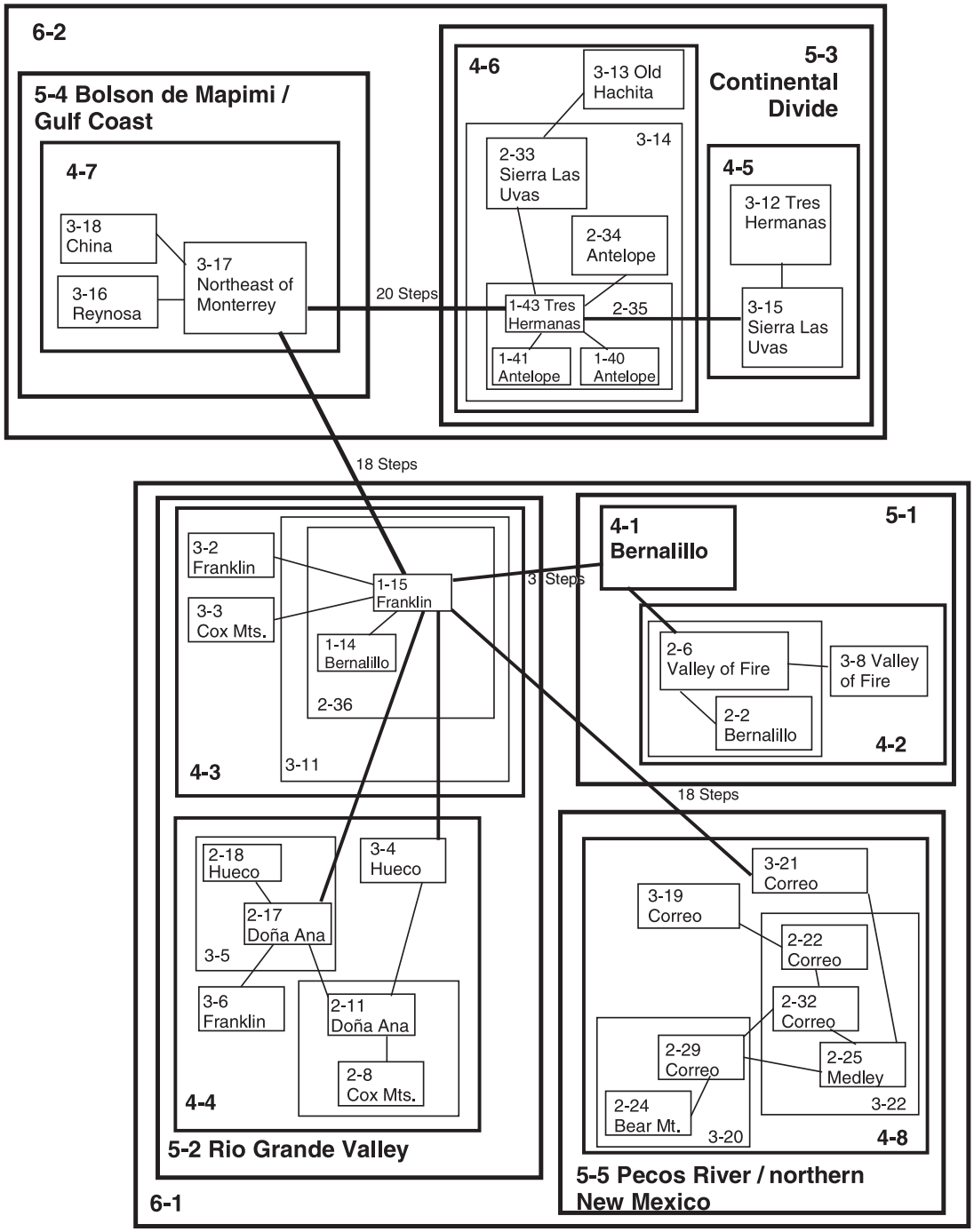

Fig. 4 Nested clades in *Moneilema armatum* showing 1-, 2-, 3-, 4-, 5-, and 6-step clades that contain both genetic and geographical variation. The number of mutational steps between major groups are shown as branch indices.

there were some exceptions to this trend, for example, within the Rio Sonora region, although there was evidence for significant population structure with some populations having diverged more than a million years ago, there was nevertheless evidence for significant gene flow between populations. For this reason, these populations could not be considered independent for purposes of analysing population growth, and were therefore pooled.

FLUCTUATE found positive growth rates in each of 12 populations analysed (two of the populations identified using MDIV contained too few sequences to be analysed using FLUCTUATE) and estimates of 'g' were significantly

Table 3 MDIV results for *Moneilema gigas*

	Rio Mayo							Rio Sonora				
	1. Alamos	2. San Carlos	3. Las Guásimas	5. San Nicolas	6. Moctezuma	7. Ures	10. Km 100	9. Huasabas	11. Cholla Bay	12. Sonoita	18. Bull's Pasture	26. Table Mts
1. Alamos	—	769 807	560 876	957 362	905 581	963 033	833 333	743 127	1 116 208	976 851	1 018 641	811 419
2. San Carlos	0.198	—	187 000	1 099 000	262 000	131 000	1 757 000	1 289 000	1 542 836	1 690 988	1 409 629	1 371 902
3. Las Guásimas	0.342	0.246	—	1 157 000	449 000	201 000	977 000	1 029 000	1 145 582	1 129 891	1 187 873	1 349 058
5. San Nicolas	0.342	0.018	0.018	—	132 000	1 431 000	1 773 00	413 000	1 862 813	1 058 823	768 175	929 076
6. Moctezuma	0.084	0.21	0.09	0.312	—	441 000	725 000	848 000	1 430 751	1 678 947	1 199 329	1 414 266
7. Ures	0.306	1.176	1.692	0.102	1.074	—	85 000	835 000	1 459 009	2 043 230	1 191 300	881 105
10. Km 100	0.204	0.006	0.006	0.006	0.138	2.754	—	1 170 000	1 134 298	1 776 254	1 209 259	987 581
9. Huasabas	0.138	0.006	0.006	0.102	0.024	0.048	0.006	—	1 553 191	1 347 207	1 707 590	1 381 112
11. Cholla Bay	0.084	0.012	0.012	0.018	0.018	0.012	0.006	0.006	—	331 832	334 713	228 631
12. Sonoita	0.09	0.006	0.006	0.03	0.006	0.012	0.012	0.018	0.102	—	9 057	205 669
18. Bull's Pasture	0.198	0.012	0.006	0.072	0.006	0.042	0.006	0.006	0.348	2.568	—	25 531
26. Table Mts	0.186	0.006	0.006	0.102	0.006	0.012	0.006	0.012	0.414	1.428	2.352	—
21. Black Mts	0.606	0.024	0.018	0.036	0.006	0.012	0.018	0.018	1.02	1.47	0.546	1.236
14. Baboquivari	0.156	0.006	0.012	0.138	0.006	0.018	0.012	0.006	0.216	1.38	0.558	0.006
19. Altar Valley	0.27	0.018	0.006	0.006	0.012	0.012	0.006	0.006	0.264	1.542	0.282	0.378
13. Sherriff's Mesa	0.156	0.006	0.042	0.036	0.012	0.006	0.048	0.018	0.228	1.104	0.042	0.456
15. Florida Canyon	0.096	0.012	0.006	0.018	0.006	0.012	0.03	0.006	0.396	0.87	0.324	0.456
16. Box Canyon	0.03	0.006	0.006	0.006	0.018	0.006	0.006	0.006	0.096	0.09	0.018	0.018
22. CSP	0.18	0.012	0.018	0.006	0.018	0.012	0.036	0.012	0.014	1.038	0.024	0.012
24. Oracle	0.366	0.018	0.024	0.006	0.012	0.006	0.024	0.012	0.384	1.566	0.018	0.060
23. Biosphere	0.12	0.006	0.012	0.084	0.006	0.03	0.018	0.012	0.144	1.104	0.018	0.048
27. Willowsprings	0.078	0.012	0.006	0.024	0.006	0.024	0.006	0.006	0.102	0.057	0.012	0.144

	Ajo Mts			Altar Valley				Santa Rita Mts	Santa Catalina Mts
	21. Black Mt	14. Baboquivari	19. Altar Valley	13. Sherriff's Mesa	15. Florida	16. Box Canyon	22. CSP	24. Oracle	23. Biosphere II	27. Willowsprings
1. Alamos	605 370	752 500	1 008 024	986 111	2 206 252	852 160	554 259	703 703	1 125 617	965 370
2. San Carlos	1 342 758	1 303 676	1 787 094	1 604 484	1 585 462	1 949 233	1 735 622	1 506 074	1 522 424	1 390 672
3. Las Guásimas	885 600	1 333 411	1 718 775	1 087 190	1 448 780	1 226 094	1 596 990	999 852	1 223 220	1 566 374
5. San Nicolas	1 267 582	1 817 758	1 125 600	1 156 133	1 442 681	1 054 252	519 824	761 142	634 549	919 076
6. Moctezuma	929.301	1 169 884	1 852 525	1 197 497	1 439 554	1 341 317	1 086298	1 284 457	1 582 476	1 536 652
7. Ures	1 113 416	1 429 100	1 658 748	1 145 644	1 346 756	1 248 644	1 335 822	1 163 644	1 105 950	980 777
10. Km 100	1 057 011	1 124 831	1 222 745	1 095 987	1 184 388	1 044 202	898 255	1 456 127	913 627	1 080 080
9. Huasabas	1 208 583	1 386 086	2 007 787	1 765 527	1 637 733	1 673 364	1 371 942	1 734 098	1 399 876	1 439 826
11. Cholla Bay	173 140	551 779	301 111	419 611	323 782	213 052	217 211	244 345	175 906	331 832
12. Sonoita	217 813	132 436	326 701	132 155	150 857	337 346	192 166	172 924	136 415	212 815
18. Bull's Pasture	205 220	246 037	270 944	288 127	128 356	355 264	296 312	294 407	225 392	445 718
26. Table Mts	124 127	312 451	295 698	181 582	118 021	159 354	242 967	112 129	215 225	168 169
21. Black Mts	—	2 694	267 208	193 607	156 213	167 833	224 376	159 772	199 139	148 690
14. Baboquivari	2.916	—	2 688	39 449	197 821	360 887	237 475	223 873	194 914	487 551
19. Altar Valley	1.062	2.976	—	6 365	302 802	205 268	238 465	297 130	290 653	354 099
13. Sherriff's Mesa	1.65	1.434	2.346	—	305 203	295 186	192 706	215 863	337 021	563 829
15. Florida Canyon	1.266	0.516	0.306	0.96	—	75 600	206 198	147 900	139 145	123.564
16. Box Canyon	0.03	0.006	0.006	0.006	1.434	—	228 454	203 020	94 406	127 205
22. CSP	0.054	0.006	0.006	0.078	0.144	0.006	—	10 042	2 932	4 661
24. Oracle	0.228	0.036	0.504	0.12	0.216	0.006	2.712	—	15 113	7 414
23. Biosphere	0.066	0.018	0.078	0.066	0.264	0.018	1.59	0.726	—	44 424
27. Willowsprings	1.28	0.03	0.09	0.036	0.324	0.324	2.982	2.91	2.64	—

Upper triangle = divergence time; Lower triangle = M.

Table 4 MDIV results for *Moneilema armatum*

	Contintental Divide			Bolson de Mapimi						Pecos River	Rio Grande				
	40. Tres Hermanas	38. Antelope	43. Las Uvas	29. Durango	30./33. Monterrey/ Monclova	31. China	32. Reynosa	34./35. Davis Mts	45. Correo	41. Hueco Mts	36. Cox Mts	37. Franklin Mts	42. Dona Ana Mts	44. Valley of Fire	46. Bernalillo
40. Tres Hermanas	—	94 000	101 000	1 904 264	1 653 193	1 490 463	1 669 061	3 219 447	3 237 471	2 890 858	2 972 288	4 069 887	3 069 069	4 317 379	3 594 666
38. Antelope	0.48	—	151 000	1 273 677	1 394 267	1 453 305	2 454 655	5 802 150	3 663 761	2 499 937	3 510 634	4 112 958	4 093 882	3 034 358	3 945 310
43. Las Uvas	0.24	0.44	—	1 306 168	1 000 912	1 092 006	1 794 682	5 154 630	4 780 983	3 087 740	2 494 950	5 679 041	3 465 889	4 495 991	4 974 237
29. Durango	0.03	0.036	0.156	—	1 081 729	1 983 257	2 462 354	2 189 426	2 591 542	1 987 764	1 664 229	2 373 648	2 295 132	2 695 353	2 694 124
30./33. Monterrey/Monclova	0.012	0.006	0.024	0.18	—	1 57 000	211 000	3 691 525	2 150 583	2 532 357	2 538 502	7 775 917	3 018 298	5 140 796	1 414 436
31. China	0.006	0.006	0.072	0.012	2.84	—	232 000	1 712 533	1 975 566	2 888 372	1 806 645	3 167 932	3 193 473	2 371 604	1 628 240
32. Reynosa	0.012	0.012	0.03	0.084	0.12	0.084	—	3 804 301	3 549 477	2 816 698	3 001 038	5 557 213	5 156 470	3 676 676	1 823 322
34./35. Davis Mts	0.012	0.006	0.012	0.006	0.006	0.018	0.006	—	47 000	1 440 000	1 011 000	985 000	1 435 000	1 510 000	918 000
45. Correo	0.006	0.018	0.006	0.03	0.006	0.018	0.006	2.958	—	1 314 000	1 180 000	1 725 000	1 492 000	1 735 000	1 565 000
41. Hueco Mts	0.006	0.006	0.006	0.042	0.012	0.018	0.018	0.006	0.012	—	195 000	163 000	90 000	177 000	149 000
36. Cox Mts	0.006	0.006	0.012	0.048	0.036	0.048	0.024	0.012	0.006	2.79	—	364 000	79 000	261 000	270 000
37. Franklin Mts	0.012	0.006	0.018	0.036	0.006	0.006	0.006	0.006	0.012	1.518	0.228	—	20 000	257 000	371 000
42. Dona Ana Mts	0.006	0.006	0.012	0.036	0.006	0.006	0.012	0.006	0.006	0.38	1.57	2.924	—	156 000	77 000
44. Valley of Fire	0.006	0.006	0.024	0.054	0.006	0.042	0.018	0.006	0.006	0.012	0.408	0.006	0.018	—	73 000
46. Bernalillo	0.006	0.018	0.024	0.036	0.018	0.054	0.036	0.12	0.018	0.564	0.432	0.126	1.172	1.48	—

Upper triangle, divergence time; Lower triangle, M.

Table 5 Population growth rate estimates determined by FLUCTUATE

Species	Region	Theta	g ($t = 1/\mu$)	r (t = 1 generation)	P (g < 0)
gigas	Alamos	0.29 ± 0.11	144.0 ± 38.7	$2.16 \times 10^{-06} \pm 5.80 \times 10^{-07}$	> 0.05
	Rio Sonora	0.51 ± 0.02	77.0 ± 2.0	$1.15 \times 10^{-06} \pm 2.95 \times 10^{-08}$	< 0.01*
	Huasabas	0.03 ± 0.002	96.7 ± 6.2	$1.45 \times 10^{-06} \pm 9.31 \times 10^{-08}$	> 0.5
	Cholla Bay	0.03 ± 0.001	126.1 ± 10.4	$1.89 \times 10^{-06} \pm 1.56 \times 10^{-07}$	> 0.5
	Ajo Mts	0.13 ± 0.03	234.0 ± 23.7	$3.51 \times 10^{-06} \pm 3.55 \times 10^{-07}$	< 0.05*
	Altar Valley	0.77 ± 0.30	432.0 ± 58.3	$6.48 \times 10^{-06} \pm 8.75 \times 10^{-07}$	< 0.01*
	Santa Ritas	0.08 ± 0.004	205.3 ± 3.5	$3.08 \times 10^{-06} \pm 5.17 \times 10^{-08}$	0.05*
	Catalinas	0.49 ± 0.24	926.6 ± 265	$1.39 \times 10^{-05} \pm 3.98 \times 10^{-06}$	< 0.01*
armatum	Continental Divide	0.08 ± 0.006	213.3 ± 12.3	$3.20 \times 10^{-06} \pm 1.85 \times 10^{-07}$	0.01*
	Bolson de Mapimi	0.65 ± 0.055	570.8 ± 37.4	$8.56 \times 10^{-06} \pm 5.61 \times 10^{-07}$	< 0.05*
	Pecos River	0.22 ± 0.03	374.0 ± 49.6	$5.61 \times 10^{-06} \pm 7.45 \times 10^{-07}$	< 0.01*
	Rio Grande	0.18 ± 0.005	40.8 ± 1.4	$6.12 \times 10^{-07} \pm 2.14 \times 10^{-08}$	< 0.01*

'g' is the population growth rate relative to the neutral mutation rate. 'r' is the per generation growth rate.

Table 6 Fu's F_S for each region

Species	Population	Fu's F_S	P
gigas	Alamos	1.24	0.475
	Rio Sonora	−9.93	< 0.001*
	Huasabas	0.12	0.286
	Cholla Bay	−2.22	0.062
	Ajo Mts	−3.93	0.016*
	Altar Valley	−1.55	0.125
	Santa Ritas	−13.56	< 0.001*
	Catalinas	−10.36	< 0.001*
armatum	Continental Divide	−6.16	0.009*
	Bolson de Mapimi	−0.80	0.21
	Pecos River	−3.23	0.03*
	Rio Grande	−8.88	0.001*

greater than zero in nine of these (see Table 5). The sign test indicates that finding positive values of 'g' across all 12 independent populations by chance would be highly unlikely ($P = 0.000244$). The more conservative statistic, Fu's F_S, found evidence of population growth in only 10 of 12 groups; seven of these were significantly different from the expectations under constant population size (Table 6). However, the sign test indicates that finding negative values of F_S for 10 of 12 populations is still a highly significant result ($P = 0.016$).

Discussion

Phylogenetic analyses revealed similar phylogeographical patterns in both of these species. For both *Moneilema gigas* and *Moneilema armatum*, phylogenetic analysis suggests successive northward movement (Figs 1 and 2), and populations on the northern edges of both the Sonoran and Chihuahuan deserts are derived with respect to populations in putative refugia. Bootstrap analysis and Bayesian posterior probabilities showed strong support for this pattern.

However, the divergence time estimates output by MDIV suggest that the apparent northward expansions in these species are considerably older than the end of the last glacial period, dating to approximately 1.5 Myr, perhaps reflecting increasing global aridity and expanding desert environments throughout the Pliocene and Pleistocene (Axelrod 1979). Nevertheless, there is a notable difference in divergence times between the northern and southern populations; divergence times within the northern regions in *M. gigas* were quite low, generally in the range of 100 000 years, and an order of magnitude lower than the divergence times between regions, suggesting that these areas were invaded more recently, perhaps during the last interglacial. However, within *M. armatum* there is evidence for a relatively ancient divergence between the Rio Grande and Pecos River regions, and southern populations in both species showed a much wider range of divergence times. In *M. gigas*, there is evidence for deep divergences between many of the populations within the Rio Yaqui and Rio Sonora valleys, suggesting that these populations may have been extant in their current locations for a very long period of time. Similarly, the populations of *M. armatum* from the Bolson de Mapimi have been differentiated from all other Chihuahuan Desert populations for at least 1.6 Myr, suggesting that it did not serve as a source for the repopulation of desert regions after the end of the last glacial, as has been argued by previous authors (Wells 1977; Van Devender & Burgess 1985). However, it is important to note that as a result of the stochasticity of the coalescent process, there will be considerable variation between loci in the time to coalescence, and so estimates of timing drawn from any single locus have the potential to be misleading.

However, although the data indicate that these species have been present in the northern regions for at least the

last 100 000 years, the coalescent analyses do suggest that global climate changes had a significant effect on the population dynamics and distribution of these species. There is strong evidence from the coalescent data for independent population growth (and perhaps local range expansions) in multiple discreet populations from across the ranges of these two species. Each of the populations analysed using FLUCTUATE shows evidence of population growth, and in nine of the 12 populations these results were highly significant. It is extremely unlikely that all of these populations would have undergone similar changes in population size by chance alone, and the sign test indicates that this is a highly significant result. It seems likely therefore that these demographic changes had a common underlying cause.

Although the coalescent models used here to analyse population growth generally assume panmixia, there was evidence for significant structure within some regions. Nevertheless, the decision to pool these populations for analysis should not have biased the analyses in favour of finding population growth. Indeed, by combining partially isolated populations, we sampled more ancient coalescent events, making it less likely that we would find evidence of population expansion.

The NCAs appear to corroborate the inferences drawn from the coalescent analyses, and provide evidence of range expansions that accompanied changes in population size. Although insufficient geographical sampling in some areas makes it difficult to draw firm conclusions from the NCAs, in both *M. gigas* and *M. armatum* there is evidence for a past history of range fragmentation, suggesting that these species have undergone range expansion following some time in refugia. Similarly, within populations of *M. armatum* from the Rio Grande and the Pecos River, there was evidence of contiguous range expansion. The results are consistent with these species having been previously widespread, perhaps during past interglacial periods, and having undergone range shifts coincident with Pleistocene glacial/interglacial cycles.

However, some caution in interpreting the results of these analyses is warranted. As pointed out by Knowles & Maddison (2003), NCA does not provide statistical measures of support for alternative biogeographical histories, and their coalescent simulations suggested that NCA may not reliably infer the actual demographic histories of populations. However, recent evaluation of the performance of NCA in reconstructing the biogeographical histories of groups where strong *a priori* evidence supports specific biogeographical scenarios found that NCA rarely produced erroneous reconstructions of those histories (Templeton 2004). Although we agree with Knowles & Maddison's (2003) assessment that NCA does not allow measures of the relative support for alternative biogeographical scenarios, and therefore is not as statistically rigorous as might be hoped, we feel that in this case the NCAs had considerable utility in that they takes into account important information about of the spatial distribution of haplotypes that could not be considered in coalescent-based tests. Furthermore, although it seems likely that there might be circumstances in which NCA would be positively misleading, in this case the results are consistent with both coalescent and phylogenetic analyses. Further evaluation of the utility of NCA therefore seems warranted.

Conclusions

The phylogenetic, nested clade, and coalescent analyses together present a detailed and nuanced picture of the biogeographical histories in these species. The results of the coalescent analyses using FLUCTUATE provide strong, population-genetic and statistical evidence for population growth and range expansion in warm-desert species from multiple independent source populations, coincident with Pleistocene climate changes. This is a compelling, independent confirmation of an expansion of desert ecosystems that had previously been suggested by packrat midden and pollen core studies (Van Devender 1990a, b; Thompson & Anderson 2000).

However, the estimated divergence time between populations suggest that localized population isolates may have persisted across this region during Pleistocene glaciations, and that modern desert species may have reached their current distributions by dispersing from multiple local refugia. Additionally, these range changes may have been superimposed on an older history of northward expansion; the NCA suggest a history of range fragmentation, and there is a northward progression in the phylogeographical patterns in both of these species that may reflect a gradual advance of desert ecosystems from the tropics into higher latitudes throughout the Pleistocene and upper Pliocene. This gradual expansion of desert ecosystems might have been repeatedly interrupted by intermittent glacial episodes that occurred throughout the mid and upper Pleistocene (Paillard 1998). The overall biogeographical history of these species, and perhaps that of the American deserts as a whole, must therefore be a complex one, involving repeated range expansions and contractions, perhaps with desert ecosystems achieving ever more northern distributions during each successive interglacial.

These results also have interesting implications for the question of the age of the Sonoran and Chihuahuan desert ecosystems. Within both *Moneilema gigas* and *Moneilema armatum*, the deepest divergences are very old, 1.5 Myr in *M. gigas* and 2–3 Myr in *M. armatum*. If these species have been restricted to true desert environments, as they are now, throughout their history, then the age estimates suggest that desert ecosystems have been extant since the

Pliocene, and that the Sonoran and Chihuahuan deserts diverged more than 3 Ma.

Acknowledgements

We wish to thank the Coronado, Gila, and Cibola National Forests, Organ Pipe Cactus National Monument, and the Mexican Secretary of the Environment, and Natural Resources for granting permission to collect insects and conduct research within their jurisdictions (USDA Permit # 2075–01; USNPS Permit # ORPI 00–35; Mexico SRE Permit # DAN-03200; Mexico SEMARNAT Permit # DOO 02–2916). Dr Rick Brusca, Wendy Moore, Nelia Padilla, John-Migue and Dylan Wilmsen, and Derrick Zwickl assisted during field collections. Molly Moore assisted with PCR and DNA sequencing for this project. We are grateful to Professors David Baum, Tony Burgess, Naomi Pierce, Kerry Shaw, Tom Van Devender, and John Wakeley for providing valuable discussion during the development of this project, and to the members of the Farrell, Pellmyr, and Sullivan Laboratories for reading drafts of this manuscript. We would also like to thank three anonymous reviewers for extremely helpful and thoughtful critiques of this study. Funding for this project was provided by the Putnam Expedition fund to the MCZ and the NSF Doctoral Dissertation Improvement Grant to C. I. Smith (Award # 0073291).

Supplementary material

The supplementary material is available from http://www.blackwellpublishing.com/products/journals/suppmat/MEC/MEC2472/MEC2472sm.htm

Fig. S1 Adams' consensus of all equally parsimonious trees with the maximum likelihood trees and Bayes consensus tree for *Moneilema gigas* showing major phylogeographical regions. Nodal indices are bootstrap/Bayes posterior probabilities.

Fig. S2 Adams' consensus of all equally parsimonious trees with the maximum likelihood trees and Bayes consensus tree for *Moneilema armatum* showing major phylogeographical regions. Nodal indices are bootstrap/Bayes posterior probabilities.

References

Axelrod DI (1979) *Age and Origin of Sonoran Desert Vegetation*. California Academy of Sciences, San Francisco.

Ayoub N, Riechert SE (2004) Molecular evidence for Pleistocene glacial cycles driving diversification of a North American desert spider, *Agelenopsis aperta*. *Molecular Ecology*, **13**, 3453–3465.

Brown D (1994) *Biotic Communities: Southwestern United States and Northwestern Mexico*. University of Utah Press, Salt Lake City.

Clement M, Posada D, Crandall K (2000) TCS: a computer program to estimate gene genealogies. *Molecular Ecology*, **9**, 1657–1660.

Daniel WW (1991) *Biostatistics, A Foundation for Analysis in Health Sciences*. J Wiley and Sons, New York.

Darwin C (1859) *The Origin of Species*. John Murray, London.

Elias SA, Van Devender TR (1992) Insect fossil evidence of late Quaternary environments in the northern Chihuahuan Desert of Texas and New Mexico: comparisons with the paleobotanical record. *Southwestern Naturalist*, **37**, 101–116.

Elias SA, Van Devender TR, De Baca R (1995) Insect fossil evidence of late glacial and Holocene environments in the Bolson de Mapimi, Chihuahuan Desert, Mexico: comparisons with the paleobotanical record. *Palaios*, **10**, 454–464.

Farrell BD (1998) Inordinate fondness explained: why are there so many beetles? *Science*, **281**, 555–559.

Farrell BD (2001) Evolutionary assembly of the milkweed fauna: cytochrome oxidase I and the age of *Tetraopes* beetles. *Molecular Phylogenetics and Evolution*, **18**, 467–478.

Farrell BD, Dussourd DE, Mitter C (1991) Escalation of plant defense: do latex and resin canals spur plant diversification? *American Naturalist*, **138**, 881–900.

Fu YX (1997) Statistical tests of neutrality of mutations against population growth, hitchhiking and background selection. *Genetics*, **147**, 915–925.

Huelsenbeck JP, Ronquist F (2001) MRBAYES: Bayesian inference of phylogeny. *Bioinformatics*, **17**, 754–755.

Issac NJ, Agapow PM, Harvey PH, Purvis A (2003) Phylogenetically nested comparisons for testing correlates species richness: a simulation study of continuous variables. *Evolution*, **57**, 18–26.

Klicka J, Zink RM (1999) Pleistocene effects on North American songbird evolution. *Proceedings of the Royal Society of London. Series B, Biological Sciences*, **266**, 695–700.

Knapp S, Mallett J (2003) Refuting refugia? *Science*, **300**, 71–72.

Knowles L, Maddison W (2003) Statistical phylogeography. *Molecular Ecology*, **11**, 2623–2635.

Kuhner M, Yamamato J, Felsenstein J (1998) Maximum-likelihood estimation of population growth rates based on the coalescent. *Genetics*, **149**, 429–434.

Lessa E, Cook JA, Patton JL (2003) Genetic footprints of demographic expansion in North America, but not Amazonia, during the late Quaternary. *Proceedings of the National Academy of Sciences of the United States of America*, **100**, 10331–10334.

Linsley EG, Chemsak JA (1984) The Cerambycidae of North America, Part VII, no. 1: *Taxonomy and Classification of the Subfamily Lamiinae, Tribes Parmenini Through Acanthoderini*. University of California Press, Berkeley.

MacKay WP, Elias SA (1992) Late Quaternary ant fossils from packrat middens (Hymenoptera: Formicidae): implications for climatic change in the Chihuahuan Desert. *Psyche*, **99**, 169–182.

Maddison WP, Maddison D (2001) MACCLADE. Sinauer, Sunderland.

Mayr E (1942) *Systematics and the Origin of Species*. Harvard University Press, Cambridge.

Mitter C, Farrell B, Wiegmann B (1988) The phylogenetic study of adaptive zones: has phytophagy promoted insect diversification? *American Naturalist*, **132**, 107–128.

Morafka DJ, Adest GA, Reyes LM (1992) Differentiation of North American deserts: a phylogenetic evaluation of a vicariance model. In: *Biogeography of Mesoamerica: Proceedings of a Symposium* (eds Darwin SP, Welden AL), pp. 195–226. Tulane UP, New Orleans.

Nielsen R, Wakeley J (2001) Distinguishing migration from isolation: a Markov chain Monte Carlo approach. *Genetics*, **158**, 885–896.

Paillard D (1998) The timing of Pleistocene glaciations from a simple multiple-state climate model. *Nature*, **391**, 378–381.

Palumbi SR (1996) The polymerase chain reaction. In: *Molecular Systematics*, 2nd edn (eds Hillis D, Moritz C, Mable BK), pp. 205–247. Sinauer, Sunderland.

Posada D, Crandall KA (1998) MODELTEST: testing the model of DNA substitution. *Bioinformatics*, **14**, 817–818.

Posada D, Crandall KA, Templeton AR (2000) GEODIS: a program for the cladistic nested analysis of the geographical distribution of genetic haplotypes. *Molecular Ecology*, **9**, 487–488.

Raske AG (1966) *Taxonomy and Bionomics of the Genus Moneilema (Coleoptera: Cerambycidae)*. University of California, Berkeley.

Riddle BR, Hafner DJ, Alexander LF (2000a) Comparative phylogeography of Baileys' pocket mouse (*Chaetodipus baileyi*) and the *Peromyscus eremicus* species group: historical vicariance of the Baja California Peninsular Desert. *Molecular Phylogenetics and Evolution*, **17**, 161–172.

Riddle BR, Hafner DJ, Alexander LF (2000b) Phylogeography and systematics of the *Peromyscus eremicus* species group and the historical biogeography of North American warm regional deserts. *Molecular Phylogenetics and Evolution*, **17**, 145–160.

Schneider S, Rosselli D, Excoffier L (2000) *ARLEQUIN VERSION 2.000: a software for population genetics analysis*. Genetics and Biometry Laboratory. University of Geneva, Geneva, Switzerland.

Smith CI, Farrell BD, (In Review) Phylogeography of the longhorn cactus beetle *Moneilema appressum* LeConte Coleoptera: Cerambycidae: was the differentiation of the Madrean sky-islands driven by Pleistocene climate changes? *Molecular Ecology*.

Sunnucks P, Hales DF (1996) Numerous transposed sequences of mitochondrial cytochrome oxidase 1–11 in aphids of the genus *Sitobion* (Hemiptera: Aphididae). *Molecular Biology and Evolution*, **13**, 510–524.

Swofford D (2002) *PAUP*: Phylogenetic Analysis Using Parsimony*. . Sinauer, Sunderland, Massachusetts.

Templeton AR (1998) Nested clade analyses of phylogeographic data: testing hypotheses about gene flow and population history. *Molecular Ecology*, **7**, 381–397.

Templeton AR (2004) Statistical phylogeography: methods of evaluating and minimizing errors. *Molecular Ecology*, **13**, 789–809.

Templeton AR, Sing CF (1993) A cladistic analysis of phenotypic association with haplotypes inferred from restriction endonuclease mapping IV: nested analyses with cladogram uncertainty and recombination. *Genetics*, **134**, 659–669.

Templeton AR, Boerwinkle E, Sing CF (1987) A cladistic analysis of phenotypic association with haplotypes inferred from restriction endonuclease mapping I: basic theory and an analysis of alcohol dehydrogenase activity in *Drosophila*. *Genetics*, **117**, 343–351.

Thompson RS, Anderson KH (2000) Biomes of western North American at 18 000, 6 000, and 0, ^{14}C yr BP reconstructed from pollen and packrat midden data. *Journal of Biogeography*, **27**, 555–584.

Van Devender TR (1990a) Late Quaternary vegetation and climate of the Chihuahuan Desert, United States and Mexico. In: *Packrat Middens: the Last 40 000 Years of Biotic Change* (eds Betancourt J, Van Devender TR, Martin PS), pp. 104–133. University of Arizona Press, Tucson.

Van Devender TR (1990b) Late Quaternary vegetation and climate of the Sonoran desert, United States and Mexico. In: *Packrat Middens: the Last 40 000 Years of Biotic Change* (eds Betancourt J, Van Devender TR, Martin PS), pp. 134–162. University of Arizona Press, Tucson.

Van Devender TR, Bradley GL (1994) Quaternary amphibians and reptiles from Maravillas Canyon Cave, Texas, with discussion of the biogeography and evolution of the Chihuahuan Desert herpetofauna. In: *Herpetology of the North American Deserts Proceedings of a Symposium* (eds by Brown PR, Wright JW), pp. 23–54. Serpent's Tale Books, Excelsior.

Van Devender TR, Burgess TL (1985) Late Pleistocene woodlands in the Bolson de Mapimi: a refugium for the Chihuahuan Desert biota? *Quaternary Research*, **24**, 346–353.

Wallace AR (1862) Narrative of a search after birds of paradise. *Proceedings of the Zoological Society of London*, 153–161.

Wares JP, Cunningham CW (2001) Phylogeography and historical ecology of the North Atlantic intertidal. *Evolution*, **55**, 2455–2469.

Wells PV (1977) Postglacial origin of the present Chihuahuan desert less than 11 500 years ago. *Transactions of the symposium on the Biological Resources of the Chihuahuan Desert Region, United States and Mexico* (eds by Wauer RH, Riskind DH), pp. 67–83. US Department of the Interior, National Park Service, Washington, D.C.

Wilf P, Cúneo NR, Kirk R, Johnson et al. (2003) High plant diversity in Eocene South America: evidence from Patagonia. *Science*, **300**, 122–125.

Chris Smith studies the role of geographic and ecological factors in determining gene flow, population structure, and species formation, and is particularly interested in the evolution of desert ecosystems. His current research examines the role of geographic structure in the diversification of yuccas and yucca moths. Brian Farrell is broadly interested in the interaction between insects and plants and the role of ecology in long-term evolutionary change, including adaptive radiations.
